

Spectroscopic confirmation of UV-bright white dwarfs from the Sandage Two-Color Survey of the Galactic Plane

Sébastien Lépine¹, P. Bergeron², and Howard H. Lanning^{3,4}

ABSTRACT

We present spectroscopic observations confirming the identification of hot white dwarfs among UV-bright sources from the Sandage Two-color Survey of the Galactic plane and listed in the Lanning (Lan) catalog of such sources. A subsample of 213 UV bright Lan sources have been identified as candidate white dwarfs based on the detection of a significant proper motion. Spectroscopic observations of 46 candidates with the KPNO 2.1m telescope confirm 30 sources to be hydrogen white dwarfs with subtypes in the DA1–DA6 range, and with one of the stars (Lan 161) having an unresolved M dwarf as a companion. Five more sources are confirmed to be helium white dwarfs, with subtypes from DB3 to DB6. One source (Lan 364) is identified as a DZ 3 white dwarf, with strong lines of calcium. Three more stars are found to have featureless spectra (to within detection limits), and are thus classified as DC white dwarfs. In addition, three sources are found to be hot subdwarfs: Lan 20 and Lan 480 are classified as sdOB, and Lan 432 is classified sdB. The remaining four objects are found to be field F star interlopers. Physical parameters of the DA and DB white dwarfs are derived from model fits.

Subject headings: solar neighborhood – stars: kinematics and dynamics – ultraviolet: stars – white dwarfs

¹Department of Astrophysics, Division of Physical Sciences, American Museum of Natural History, Central Park West at 79th Street, New York, NY 10024, USA; lepine@amnh.org

²Département de Physique, Université de Montréal, C.P. 6128, Succursale Centre-Ville, Montréal, QC H3C 3J7, Canada

³National Optical Astronomical Observatories, 940 North Cherry Avenue, Tucson, AZ, USA

⁴Visiting Astronomer, Kitt Peak National Observatory, Kitt Peak, AZ, USA

1. Introduction

Areas of the sky at low Galactic latitudes remain relatively unexplored for white dwarf stars. The Villanova catalog of spectroscopically identified white dwarfs (McCook & Sion 1999), recently updated¹, shows a dearth of objects in the Galactic latitude range $-25 < b < 25$. Yet white dwarfs should be quite numerous in the plane of the Milky Way, especially the younger and more massive hot white dwarfs associated with the young disk population. The 122 very nearby white dwarfs ($d < 20$ pc) identified by Holberg et al. (2008) appear to be distributed uniformly over the sky, which suggests relative completeness; however, ongoing surveys are turning up additional white dwarfs within this range (Subasavage et al. 2007; Lépine et al. 2009), and it is clear that the white dwarf census is significantly incomplete beyond 20 pc. Many more white dwarfs remain to be identified, particularly in the low galactic latitude regions. This is important if one is to obtain a statistically complete census within a much larger volume and to track the younger white dwarfs in local zones of recent star formation (de Zeeuw et al. 1999).

In recent years, white dwarfs have been identified in large numbers based on color cuts and/or reduced proper motion selection in deep optical surveys such as in the Sloan Digital Sky Survey (SDSS; Kilic et al. 2006; Eisenstein et al. 2006) and the CFHTLS Deep fields (Limboz et al. 2008) and also in photographic material for the GSC-II catalog (Carollo, et al. 2006). These surveys have however been covering only areas of high Galactic latitude, and have been mostly sensitive to relatively distant, old white dwarfs of the thick disk and halo (Gates et al. 2004; Vidrih et al. 2007).

Proper motion surveys remain the principal source of discovery for very nearby white dwarfs. Follow-up studies of older proper motion catalogs such as the Luyten half-second (LHS) and NLTT (Luyten 1979a,b) continue to turn up new white dwarfs (Vennes & Kawka 2003; Reid & Gizis 2005), while new proper motion surveys are filling the gaps (Ruiz & Bergeron 2001; Lépine, Rich, & Shara 2003; Scholz et al. 2004; Rowell, Kilic, & Hambly 2008). However, because high proper motion catalogs are more sensitive to nearby high velocity stars, many of the new white dwarfs are found to be associated with the Galactic halo (Scholz, Meusinger, & Jahre 2005; Lépine, Rich, & Shara 2005). White dwarfs from the young disk population are not expected to have extreme proper motions beyond 20 pc, but should be found among the thousands to millions of stars with small to moderate proper motions. White dwarfs can be identified in large catalogs of proper motion sources with the use of a reduced proper motion diagram, in which they populate a distinct locus. The identification is particularly straightforward when one uses an optical-to-infrared reduced proper motion diagrams

¹<http://www.astronomy.villanova.edu/WDCatalog/index.html>

(Lépine, & Shara 2005), where the white dwarfs are segregated from field dwarfs and subdwarfs. Unfortunately, white dwarfs fade out from all-sky infrared surveys (Two Micron All Sky Survey, DENIS) beyond a short distance range due to their low intrinsic luminosity in infrared bands.

One promising avenue is the combination of proper motion data with catalogs of UV-bright sources. Faint UV-bright sources, in particular, are unlikely to have significant proper motions unless they are white dwarfs. We have recently compiled proper motion data for UV-bright sources identified in a ~ 2000 deg² area of the Sandage two-color survey of the Galactic plane, in an attempt to identify white dwarf stars at low galactic latitudes. Our analysis indicates that a reduced proper motion diagram readily identifies candidate white dwarfs (Lanning & Lépine 2006).

In this paper, we present the results of our spectroscopic follow-up survey which confirms the white dwarf status of our UV and proper motion selected sources. Formal spectral classification is presented for 46 UV-bright sources, of which 39 are confirmed to be white dwarfs, three are hot subdwarfs, and the remaining four are field F dwarf interlopers. Target selection is described in Section 2, observations are presented in Section 3, results are analyzed in Section 4, and summarized in the conclusion (Section 5).

2. Target Selection

The Lanning catalog of UV-bright sources compiles objects with very blue $U - B$ colors, identified in the Sandage two-color survey of the Galactic plane. UV-bright sources were identified by visual scanning, in 48 of the 124 two-color photographic plates. With each plate covering a field of about 43 deg², the survey extends to about 2000 deg² of low Galactic latitude fields. The survey has produced 734 published sources, ranging in color from $U - B = 0$ to $U - B = -1.5$ (Lanning 1973, Lanning & Meakes 1994, 1995, 1998, 2000, 2001, 2004). The catalog includes seven identified cataclysmic variables, along with many verified and probable hot stars such as white dwarfs, Be stars, hot subdwarfs, and central stars of planetary nebulae. However, only a few of the published Lanning stars have formal spectral classification. Counterparts to Lanning stars were identified in the USNO-B1 catalog of Monet et al. (2003) with 213 sources found to have proper motions larger than 10 mas yr⁻¹; these have been suggested to be mostly white dwarfs within ≈ 200 pc of the Sun (Lanning & Lépine 2006). These stars were targeted for follow-up spectroscopy.

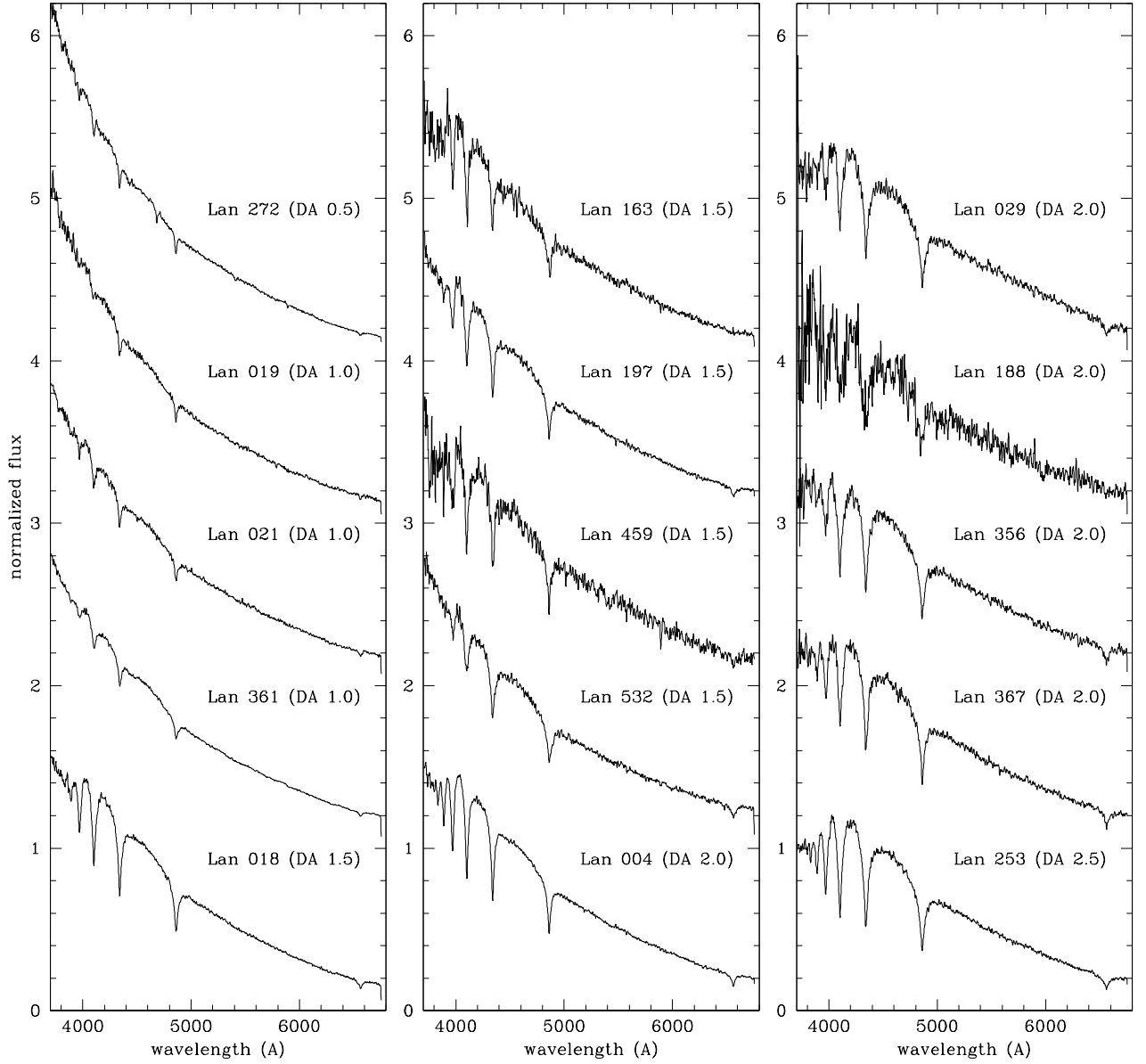


Fig. 1.— Lanning sources classified as DA white dwarfs, compact degenerates with hydrogen-line spectra. The spectrum of Lan 272 also exhibits the He II $\lambda 4686$ absorption feature and is thus classified as DAO.

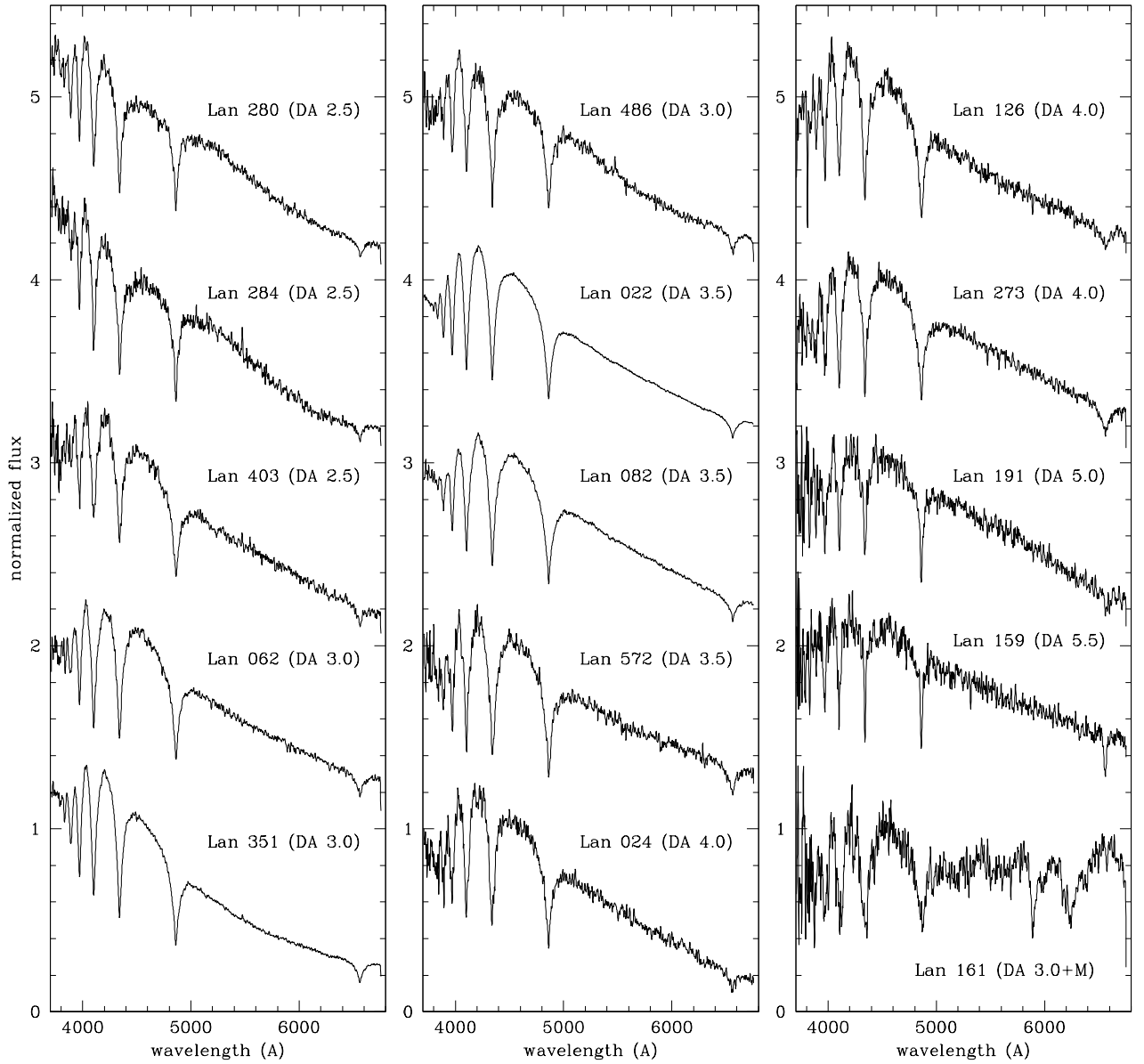


Fig. 2.— Lanning sources classified as DA white dwarfs, compact degenerates with hydrogen-line spectra. The star Lan 161 is revealed to have an unresolved M dwarf companion.

3. Observations

Observations were performed on the nights of 2007 October 15–18, from the 2.1 m telescope on Kitt Peak. In four nights, a total of 46 target stars were observed with the GoldCam CCD spectrograph. We used the “240” grism, blazed at 5500 Å, to obtain spectra with a resolution of $1.5 \text{ \AA pixel}^{-1}$. Calibration arcs of HeNeAr were observed for wavelength calibration. Four standard stars were also observed for flux calibration.

Reduction was conducted with IRAF, including standard bias correction, flat fielding, subtraction of the sky background, aperture extraction, wavelength calibration, and normalization. The resulting medium-resolution spectra are calibrated to a wavelength accuracy of 0.3 \AA .

Spectra were first examined visually and an initial classification was made based on comparison with published, spectroscopic sequences of main-sequence stars (Silva & Cornell 1992) and hot subdwarfs (Moehler et al. 1990), and with the spectroscopic atlas of white dwarfs compiled by Wesemael et al. (1993). Most sources were classified as white dwarfs of spectral class DA (hydrogen-line), DB (helium-line), and DC (featureless). Four sources were found to be consistent with main-sequence F stars; five others were found to be consistent with hot subdwarfs (sdB/sdO). Spectral subtypes for the DA and DB white dwarfs were assigned on the basis of the temperatures determined by the atmospheric model fits (see Section 3). Subtypes for the DC white dwarfs were estimated by comparing the overall spectral energy distribution with a blackbody profile. Subtypes were assigned following the general prescription of $50,400/T_{\text{eff}}$, with the resulting value rounded up to the nearest half subtype (Wesemael et al. 1993). Table 1 lists all 46 sources observed, their positions and proper motions, their magnitudes on the photographic POSS-II plates as obtained from the USNO-B1.0 catalog (Monet et al. 2003), and their assigned spectral type.

4. Comparison to previously known objects

A search of the literature found published, formal spectral subtypes for five of the stars. The subtypes are listed in Table 1 along with the bibliographic reference. The previously reported subtypes are broadly consistent with our own classification.

These stars include Lan 18, a fairly well-known DA star first classified as DA2 by Liebert & Strittmatter (1977); also Lan 020, which was first identified as an sdO by Walker (1981). In addition, six of our sources had also been previously observed by Eracleous et al. (2002), who provided a broad “spectral class” diagnostic to indicate whether the star appeared to be a hot object or not. Both Lan 19 and Lan 21 were noted to be “Hot, high

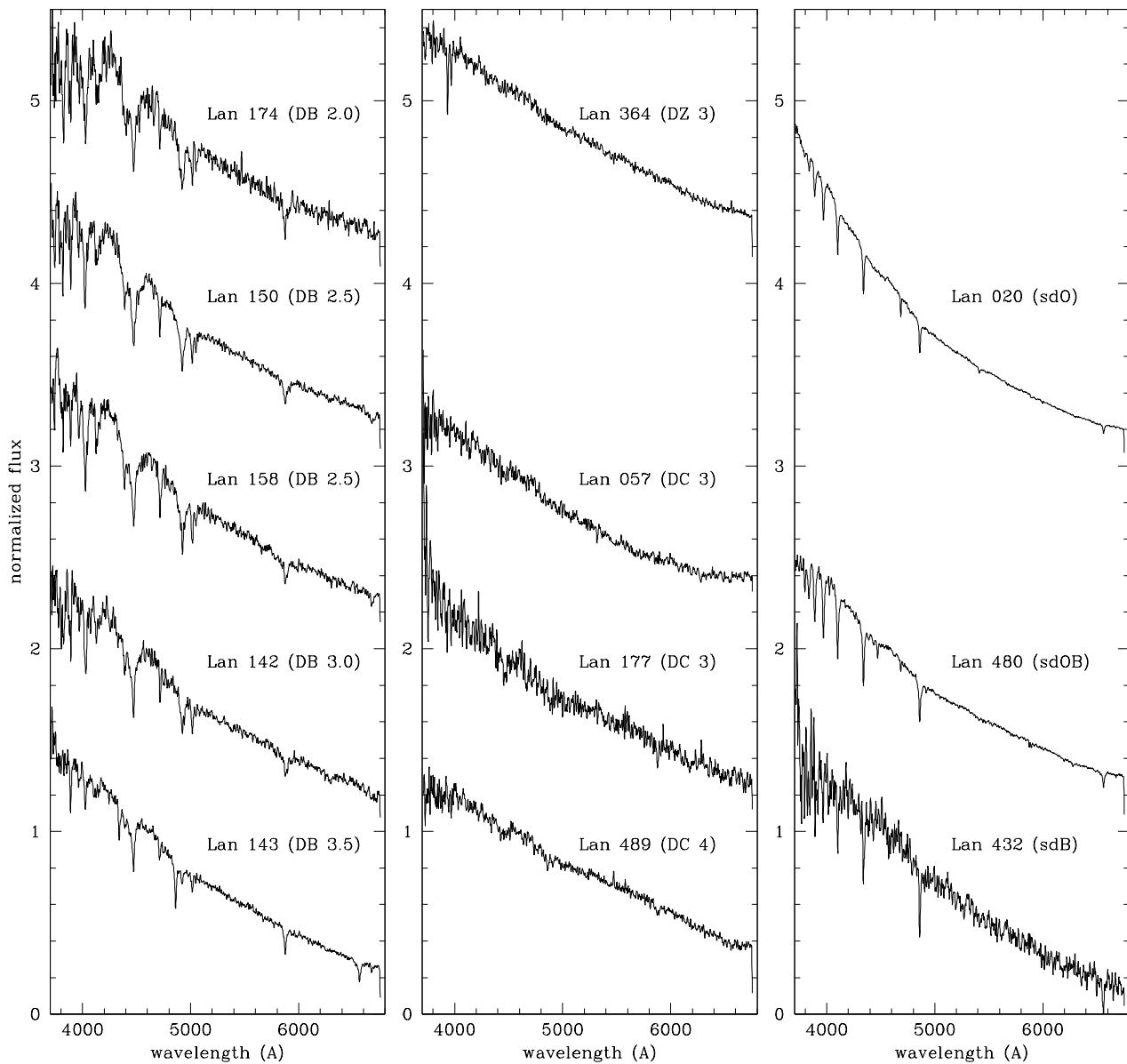


Fig. 3.— Lanning sources classified as DB, DZ, and DC white dwarfs. The DB white dwarfs have spectra dominated by neutral helium lines, while the DZ shows lines of calcium. The DC white dwarfs appear featureless to within our detection limits. Also shown are the stars we classify as hot subdwarfs (sdO and sdB), whose gravities are lower than main-sequence stars but not as extreme as in the white dwarfs.

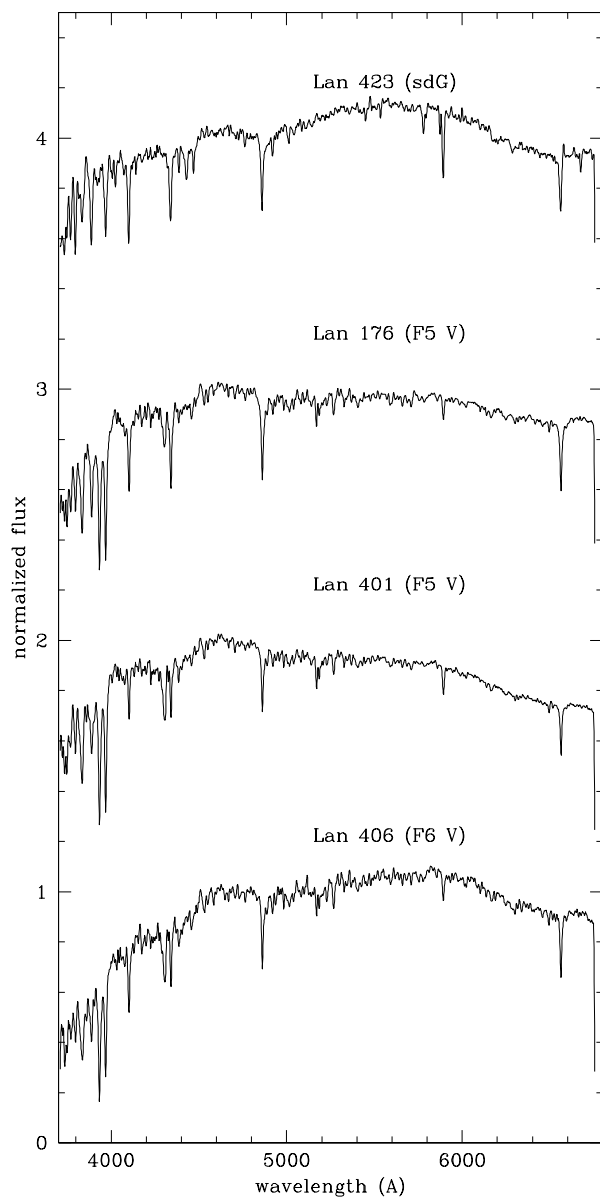


Fig. 4.— Lanning sources initially flagged as probable white dwarfs, but revealed to be field F stars. One of the sources (Lan 423) has the Na λ line as strong as H α , which would normally indicate a spectral type G, but lines of Mg λ are absent or weak. We interpret this as the star being metal poor, and classify it as a G subdwarf (sdG).

gravity?,” Lan 22 was classified as “O7-O9,” Lan 367 was classified as “B0-B3,” Lan 423 was noted to be “Early B,” Lan 401 was identified as a “late F-G,” and Lan 406 as a “late-F,” while Lan 423 was identified as “early-B” and Lan 459 was simply classified as “DA.” Those impressions are also noted in Table 1; they are generally consistent with our own spectral types.

It is also interesting that Lan 021 is associated to a possible planetary nebula by Kronberger et al. (2006). Likewise, Lan 272 was classified as a possible central star of planetary nebula by Chromey (1979).

5. Atmospheric model fits

Our model atmospheres and synthetic spectra for DA stars are described at length in Tremblay et al. (2010) and references therein; these make use, in particular, of the improved Stark profiles for the hydrogen lines developed by Tremblay & Bergeron (2009). Non-local thermodynamic equilibrium (NLTE) effects are explicitly taken into account above $T_{\text{eff}} = 20,000$ K and energy transport by convection is included in cooler models following the $ML2/\alpha = 0.8$ prescription of the mixing-length theory. Our model atmospheres and synthetic spectra for DB stars are similar to those described in Beauchamp et al. (1996), which include the improved Stark profiles of neutral helium of Beauchamp et al. (1997). Our fitting technique relies on the nonlinear least-squares method of Levenberg–Marquardt, which is based on a steepest descent method. The model spectra (convolved with a Gaussian instrumental profile) and the optical spectrum of each star are first normalized to a continuum set to unity. The calculation of χ^2 is then carried out in terms of these normalized line profiles only. Atmospheric parameters – T_{eff} , $\log g$, as well as H/He for DBA stars or He/H for DAO stars – are considered free parameters in the fitting procedure.

6. Classification and spectroscopic analysis

Spectra of the sources classified as DA (hydrogen-line) white dwarfs are displayed in Figures 1 and 2. The 28 stars show the characteristic, broad lines of the hydrogen Balmer series; Lan 272 also exhibits the He II $\lambda 4686$ absorption feature and is thus classified as a DAO star. Elements of the atmospheric model fits are reported in Table 2. The spectral subtypes listed in Table 1 are based on the model-determined effective temperatures listed here. Additionally, the star Lan 161 is revealed to be a binary star, consisting of a white dwarf with a low-mass, main sequence companion; the star displays the characteristic signature of

broad Balmer lines on the blue side, but redward of 5000 Å the spectrum clearly displays the broad molecular features usually observed in M dwarfs (Kirkpatrick, Henry, & MaCarthy 1991; Reid, Hawley, & Gizis 2005; Lépine, Rich, & Shara 2003), in particular a deep CaOH band around 6250 Å.

Spectra of the five objects classified as DB (helium-line) white dwarfs are displayed in Figure 3; the spectrum of Lan 143 also shows hydrogen lines and is thus classified DBA. Elements of the atmospheric fits are provided in Table 3 and include estimates of the hydrogen abundances, or upper limits, based on the presence or absence of H α .

Figure 3 also shows the stars with featureless spectra, which we identify as DC white dwarfs, along with the spectrum of Lan 364, which we classify as a DZ (white dwarf with traces of metal) based on detection of a Ca II $\lambda\lambda 3933 - 3968$ doublet. These stars are not suited for atmospheric model fits without accurate color information, and their physical parameters are left undetermined.

The three stars identified as hot subdwarfs also have their spectra displayed in Figure 3. All show relatively narrower lines of the hydrogen Balmer series indicative of a lower surface gravity. Their gravities are however significantly higher than in main-sequence stars.

Finally, spectra of the four objects classified as main sequence F stars are shown in Figure 4. The star Lan 423 has a spectrum consistent with a main-sequence F star, but lacks strong absorption in the extreme blue, which is interpreted to be the possible signature of a metal-poor atmosphere.

Atmospheric model fits yield estimates of the ages and masses of the DA and DB white dwarfs. Hot white dwarfs tend to be relatively young, and this is confirmed by the model fits. Figure 5 shows the location of the stars in the mass-effective temperature diagram, and compares it to theoretical isochrones. For DA stars with $T_{\text{eff}} > 30,000$ K, we use the carbon-core cooling models of Wood (1995) with thick hydrogen layers of $q(\text{H}) \equiv M_{\text{H}}/M_{\star} = 10^{-4}$ and $q(\text{He}) = 10^{-2}$, while for $T_{\text{eff}} < 30,000$ K, we use cooling models similar to those described in Fontaine et al. (2001) but with carbon–oxygen cores. For DB stars, we rely on similar models but with thin hydrogen layers of $q(\text{H}) = 10^{-10}$ representative of helium-atmosphere white dwarfs. The distribution shows that most of our stars have been in the white dwarf phase for less than 1 Gyr. Model-fits yield relatively low-masses for the youngest white dwarfs, some apparently below $0.4 M_{\odot}$, and these are most likely unresolved double degenerate binaries that are the result of common envelope evolution.

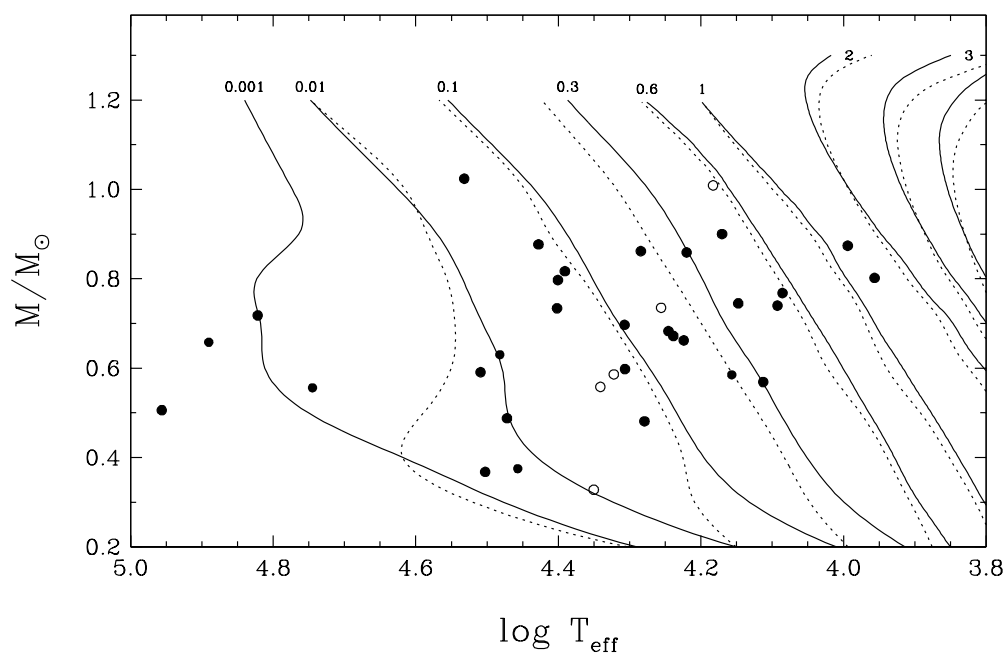


Fig. 5.— Isochrones of the white dwarf evolutionary models in the mass/effective temperature diagram. The isochrones are labeled in billions of years (Gyr); DA white dwarf isochrones are plotted as continuous lines, while the slightly different DB isochrones are plotted as dotted lines. Estimates for the white dwarfs presented in this paper are noted as filled circles for the DA white dwarfs, and as open circles for the DBs. Most of our stars are found to have been in the white dwarf phase for less than 1 billion years.

7. Kinematic analysis

By combining the measured proper motions and the distances estimated using the atmospheric model fits, we calculate transverse velocities for all the DA and DB white dwarfs. These velocities are two-dimensional vectors, which are projections of the three-dimensional motion vectors of the stars in the plane of the sky. All of our stars are located at low Galactic latitudes ($|b| < 10.0$) which means that the proper motion in the direction of the galactic coordinate b is effectively equivalent to the component of motion W (the component of velocity normal to the plane of the Galaxy.) The component of motion in the direction of l is then a combination of the components of motion U (in the direction of the Galactic center) and V (in the direction of Galactic rotation).

Generally, the components of U , V , and W can be calculated using

$$U = 4.74d(\mu_l \sin(l) - \mu_b \cos(l) \sin(b)) + V_r \cos(l) \cos(b) \quad (1)$$

$$V = 4.74d(\mu_l \cos(l) - \mu_b \sin(l) \sin(b)) + V_r \sin(l) \cos(b) \quad (2)$$

$$W = 4.74d\mu_b \cos(b) + V_r \sin(b). \quad (3)$$

For the case where radial velocities are unknown, it is possible to estimate with reasonably good accuracy the components of motion for any two pairs (UV , UW , or VW) by selecting subsamples of stars at particular locations on the sky. For example, stars with $|b| \approx 90.0$ have $\cos(b) \approx 0$ and from Equations (1) and (2) we see that the component of radial velocity becomes negligible in the calculation of both U and V . The calculated U and V components of stars near the Galactic pole will thus be reasonably accurate, even though the radial velocity component is not known a priori. Likewise, components of U and W will be a reasonably good representation for proper motion stars near $l = 90, b = 0$ or $l = 270, b = 0$, and components of V and W will be a reasonable good representation for stars near $l = 0, b = 0$ or $l = 180, b = 0$.

We thus assume all radial velocities to be zero (0.0) and estimate the components of motion in U , V , and W using Equations (1)–(3) for all the DA and DB white dwarfs in our sample. We then separate our objects into two groups: (1) stars with $45 < l < 135$ and $225 < l < 315$, and (2) stars with $135 < l < 225$ and $315 < l < 45$. The first group yields a reasonably accurate distribution in the projected UW velocity plane, while the second groups yield a reasonably good distribution in the VW plane.

We further separate the samples according to the ages derived from the model fits. Separate plots are generated for stars with estimated ages (of the white dwarf phase) of $\tau < 10^{7.5}$ yr, and stars with ages $\tau > 10^{7.5}$ yr. The separation limit corresponds to an age

of ≈ 31 Myr, and essentially sets apart the very recent white dwarfs from the rest. The velocity-space distributions are shown in Figure 6. As in Figure 5, the DA white dwarfs are represented with filled symbols, while the DB white dwarfs are shown as open symbols. The top panels show the kinematics of the very recent white dwarfs, while the bottom panels show the kinematics of the older objects. Transverse velocities are all under 70 km s^{-1} , which is largely consistent with thin disk kinematics.

An intriguing result is that the youngest white dwarfs appear to stand out in velocity space: they all show $U > 0 \text{ km s}^{-1}$, whereas the older objects tend to have $U < 0 \text{ km s}^{-1}$. The trend itself has more to do with the orientation of the proper motion vector, and does not depend much on the accuracy of the distance estimates. A position value of U signifies that the object is currently moving toward the Galactic center, while a negative value means it is moving out. The bulk of the stars in the vicinity of the Sun have $U < 0 \text{ km s}^{-1}$ (Nordstrom et al. 2004) including most of the young moving groups (Bovy, Hogg, & Roweis 2009). Our results would suggest that our youngest white dwarfs are not associated with the recent star formation in the immediate solar neighborhood. Nearby white dwarfs do appear to have a more symmetric distribution around $U = 0$ (Kawka & Vennes 2006), which is not so much at odds with our $U > 0$ trend given the small size of our sample. The trend would definitely need to be confirmed with additional data points. It could be that the very young white dwarfs in our sample are also the most luminous and the most distant, with $d \gtrsim 200 \text{ pc}$. A possible $U > 0$ trend might arise if these stars are members of more distant young moving groups, with kinematics very distinct from the local ones. A confirmation of this trend would require spectroscopic follow-up of a much larger sample of hot white dwarfs, or a search for kinematic groups beyond the current distance limit of the *Hipparcos* catalog (from which most of the local moving groups have been discovered).

Figure 7 shows the reduced proper motion diagram of the stars observed in this paper. Different symbols are used to distinguish stars of different gravity classes (circles for white dwarf, triangles for subdwarf, squares for main-sequence stars). A representative sample of 15,000 field stars with proper $\mu > 20 \text{ mas yr}^{-1}$, drawn from the USNO-B1.0 catalog (Monet et al. 2003), is shown for comparison (dots). The reduced proper motion diagram segregates the main-sequence stars from the white dwarfs and subdwarfs. In the reduced proper motion diagram, white dwarfs occupy the lower left of the stellar locus (blue stars with large reduced proper motion). The straight line in Figure 7 shows the approximate border separating the white dwarfs from the main-sequence stars, based on the observed distribution of field stars. One sees that while the majority of the white dwarfs observed in our study do indeed fall blueward of the line, some fall to the red, and would not readily be suspected to be white dwarfs based on their proper motion and optical colors alone. We suggest that the combination of a demonstrated UV excess in conjunction with a high proper

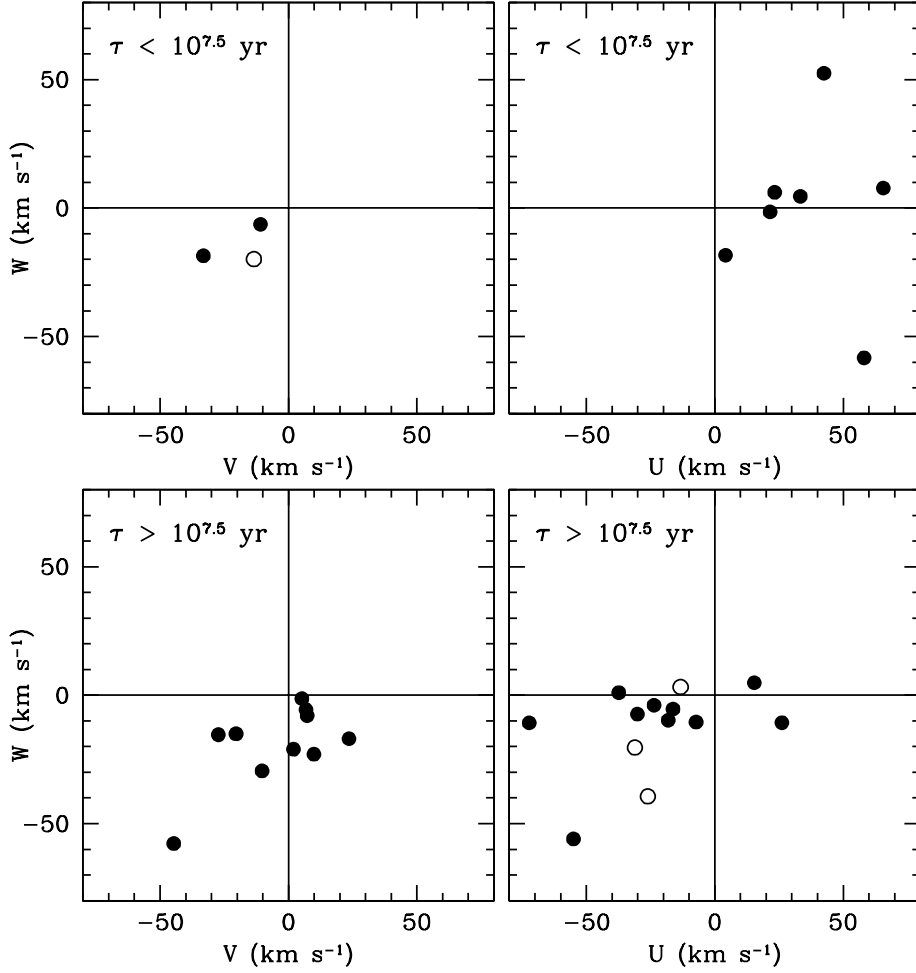


Fig. 6.— Kinematics of the DA and DB white dwarfs (filled and open circles, respectively). The left panels show the velocities in the direction of Galactic rotation (V) and normal to the plane (W) for stars located in the direction of $l \approx 0$ and $l \approx 180$. Right panels show velocities toward the Galactic center (U) and normal to the Galactic plane (W) for stars located in the direction of $l \approx 90$ and $l \approx 270$. The youngest white dwarfs are plotted in the top panels, older ones in the bottom panels. Young white dwarfs are all found to have $U > 0$ km s⁻¹ while older white dwarfs show the exact opposite trend.

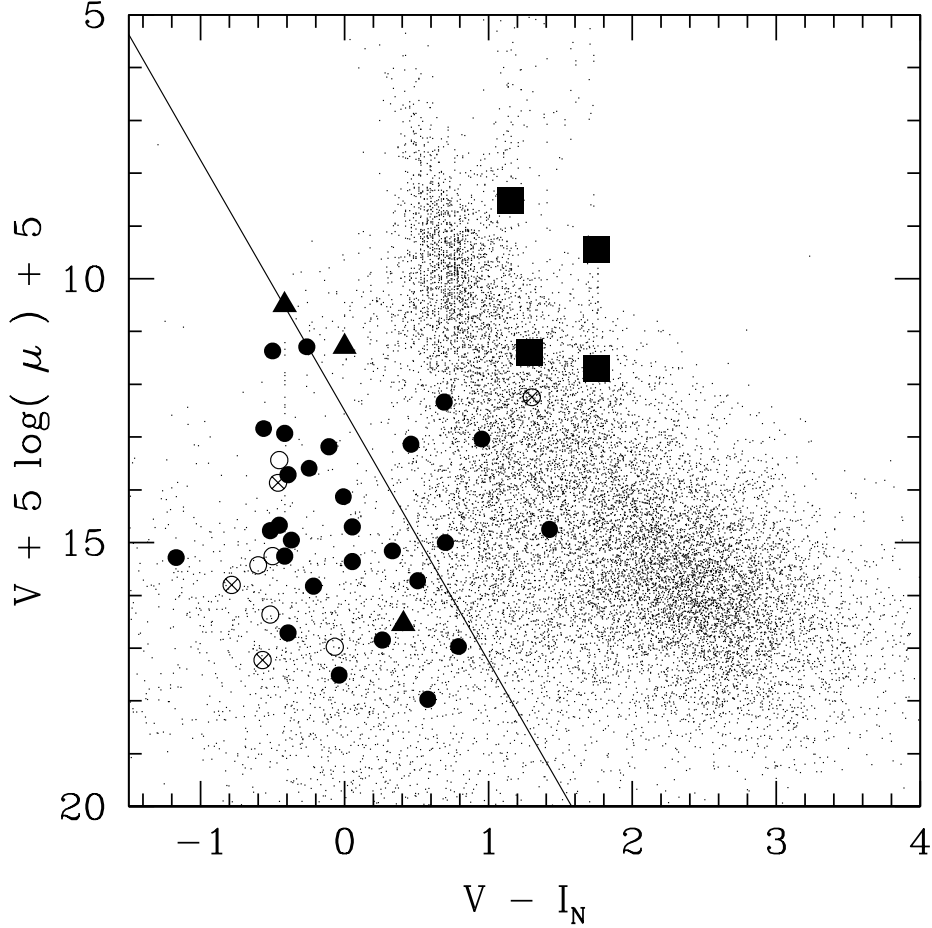


Fig. 7.— Optical-to-infrared reduced proper motion diagram of the sources observed in this paper (large symbols). A representative sample of stars with large proper motions ($\mu > 150$ " yr $^{-1}$) is shown for comparison (dots). White dwarfs are shown as circles, with filled circles representing the DA, open circles the DB, and crossed circles the DZ and DC. Hot subdwarfs (sdO/sdB) are plotted as triangles, and main-sequence stars as squares. The straight line shows a typical limit used to separate out white dwarf (lower left) from main-sequence stars of the disk and halo (upper right). Most, but not all, of our confirmed white dwarfs fall on the expected side of the line; the hot subdwarfs are blended in with the white dwarfs and cannot be readily identified in the diagram.

motion would be more efficient in identifying hot white dwarfs at low Galactic latitudes. A reduced proper motion diagram based on ultraviolet to optical colors may turn out to be the best tool.

One caveat of this method is that interstellar absorption will significantly reduce the UV brightness of stars beyond a few hundred parsecs. Selection of hot white dwarfs based on UV excess will thus work best for relatively nearby objects. The exact range over which this method will be efficient and/or reliable remains to be determined.

8. Conclusions

Our spectroscopy confirms that, as suggested in Lanning & Lépine (2006), most of the UV-bright stars from the Lanning catalog that also have large proper motions ($>10 \text{ mas yr}^{-1}$) are for the most part white dwarfs. Several more Lanning stars remain with no formal spectral classification. We predict that all the stars in the lower left region of the reduced proper motion diagram will be revealed as white dwarfs or hot subdwarfs in future spectroscopic follow-up surveys.

The identification of white dwarfs based on a combination of UV excess and proper motion holds the potential to significantly increase the census of young nearby white dwarfs. The strong predictive power for white dwarfs selected by UV excess suggests that a combination of proper motion data and broadband UV magnitudes as provided, e.g., by the *Galaxy Evolution Explorer (GALEX)* mission, such as the recent work by Vennes, Kawka, & Németh (2011), would be extremely efficient in expanding the census of nearby white dwarfs.

However, we note that the *GALEX* mission generally avoids fields at low Galactic latitudes ($|b| < 20.0$), which means that these regions will remain relatively unexplored, until UV imaging will be performed to cover those potentially rich hot white dwarf hunting grounds.

Acknowledgments

Howard H. Lanning sadly passed away in 2007 December, just a few months after carrying out the spectroscopic observations presented in this paper. He will be missed by his friends and colleagues.

We thank A. Gianninas for his fits to the two hottest white dwarfs in our sample and P. Brassard for providing us with his grid of subdwarf model spectra. S.L. was supported in this research by NSF grants AST-0607757 and AST-0908406 at the American Museum of Natural History. This work was also supported in part by the NSERC Canada and by

the Fund FQRNT (Québec). P.B. is a Cottrell Scholar of Research Corporation for Science Advancement.

REFERENCES

- Beauchamp, A., Wesemael, F., & Bergeron, P. 1997, *ApJS*, 108, 559
- Beauchamp, A., Wesemael, F., Bergeron, P., Liebert, J., & Saffer, R. A. 1996, in *ASP Conf. Ser. 96, Hydrogen-Deficient Stars*, ed. S. Jeffery & U. Heber (San Francisco, CA: ASP), 295
- Bovy, J., Hogg, D. W., & Roweis, S. T. 2009, *ApJ*, 700, 1794
- Carollo, D., et al. 2006, *A&A*, 448, 579
- Chromey, F. R. 1979, *AJ*, 84, 534
- Eisenstein, D. J., et al. 2006, *ApJS*, 167, 40
- Eracleous, M., Wade, R. A., Mateen, M., Lanning, H. H. 2002, *PASP*, 114, 207
- Fontaine, G., Brassard, P., & Bergeron, P. 2001, *PASP*, 113, 409
- Gates, E., et al. 2004, *ApJ*, 612, L129
- Holberg, J. B., Sion, E. M., Oswalt, T., McCook, G. P., Foran, S., & Subasavage, J. P. 2008, *AJ*135, 1225
- Kawka, A., & Vennes, S. 2006, *ApJ*, 643, 402
- Kilic, M., et al. 2006, *AJ*, 131, 582
- Kilkenny, D., Heber, U., & Drilling, J. S. 1988, *South Afr. Astron. Obs. Circ.*, 12, 1
- Kirkpatrick, D., Henry, T. J., & MaCarthy, D. W., Jr. 1991, *ApJS*, 77, 417
- Kronberger, M., et al. 2006, *A&A*, 447, 921
- Lanning, H. H. 1973, *PASP*, 85, 70
- Lanning, H. H., & Lépine, S. 2006, *PASP*, 118, 539
- Lanning, H. H., & Meakes, M. 1994, *PASP*, 106, 38

- Lanning, H. H., & Meakes, M. 1995, PASP, 107, 751
- Lanning, H. H., & Meakes, M. 1998, PASP, 110, 786
- Lanning, H. H., & Meakes, M. 2000, PASP, 112, 251
- Lanning, H. H., & Meakes, M. 2001, PASP, 113, 1393
- Lanning, H. H., & Meakes, M. 2004, PASP, 116, 1039
- Lépine, S., Rich, R. M., & Shara, M. M. 2003, AJ, 125, 1598
- Lépine, S., Rich, R. M., & Shara, M. M. 2005, ApJ, 633, L121
- Lépine, S., & Shara, M. M. 2005, AJ, 129, 1483
- Lépine, S., Thorstensen, J. R. & Shara, M. M. 2009, AJ, 137, 4109
- Liebert, J., & Strittmatter, P. A. 1977, ApJ, 217, 59
- Limboz, F., Karatas, Y., Kilic, M., Benoist, C., & Alis, S. 2008, MNRAS, 383, 957
- Luyten W. J. 1979a, LHS Catalogue: A Catalogue of Stars with Proper Motions Exceeding $0''.5$ annually (CDS-ViZier catalog number I/87B; MN, Univ. Minnesota)
- Luyten W. J. 1979b, New Luyten Catalogue of Stars with Proper Motions Larger Than Two Tenths of an Arcsecond (NLTT) (CDS-ViZier catalog number I/98A; MN, Univ. Minnesota)
- McCook, G. P., & Sion, E. M. 1999, ApJS, 121, 1
- Moehler, S., Richtler, T., de Boer, K. S., Dettmar, R. J., & Heber, U. 1990, A&AS, 86, 53
- Monet, D. G., et al. 2003, AJ, 125, 984, (The USNO-B1 Catalog – CDS-ViZier catalog number I/284)
- Nordstrom, B., et al. 2004, A&A, 418, 989
- Reid, I. N., & Gizis, J. E. 2005, PASP, 117, 676
- Reid, I. N., Hawley, S. L. & Gizis, J. E. 2005, AJ, 110, 1838
- Rowell, N. R., Kilic, M., & Hambly, N. C. 2008, MNRAS385, L23
- Ruiz, M. T., & Bergeron, P. 2001, ApJ, 558, 761

- Scholz, R.-D., Meusinger, H., & Jahreiss, H. 2005, *A&A*, 442, 211
- Scholz, R.-D., et al. 2004, *A&A*, 425, 519
- Silva, D. R., & Cornell, M. E. 1992, *ApJS*, 81, 865
- Subasavage, J. P., Henry, T. J., Bergeron, P., Dufour, P., Hambly, N. C., & Beaulieu, T. D. 2007, *AJ*, 134, 252
- Tremblay, P.-E., & Bergeron, P. 2009, *ApJ*, 696, 1755
- Tremblay, P.-E., Bergeron, P., Kalirai, J.S., & Gianninas, A. 2010, *ApJ*, 712, 1345
- Vennes, S., & Kawka, A. 2003, *ApJ*, 586, L95
- Vennes, S., Kawka, A., & Németh, P. 2011, *MNRAS*, 410, 2095
- Vidrih, S., et al. 2007, *MNRAS*, 382, 515
- Walker, A. R. 1981, *MNRAS*, 197, 241
- Wesemael, F., Greenstein, J. L., Liebert, J., Lamontagne, R., Fontaine, G., Bergeron, P., & Glaspey, J. W. 1993, *PASP*, 105, 761
- Wood, M. A. 1995, in 9th European Workshop on White Dwarfs, NATO ASI Series, ed. D. Koester & K. Werner (Berlin: Springer), 41
- de Zeeuw, P. T., Hoogerwerf, R., de Bruijne, J. H. J., Brown, A. G. A., & Blaauw, A. 1999, *AJ*117, 354

Table 1. Spectroscopically Classified UV-bright Sources

Name	α (J2000)	δ (J2000)	μ_α (mas yr ⁻¹)	μ_δ (mas yr ⁻¹)	m_B (mag)	$U - B$ (mag)	B_J (mag)	R_F (mag)	I_N (mag)	Sp. Type (Old)	Sp. Type (New)
Lan 004	01 26 08.8	+69 01 55.3	-22	8	16	-0.9	15.9	16.3	16.5		DA 2.0
Lan 018	18 47 39.1	+01 57 39.1	-2	-74	12	-0.9	12.9	13.1	12.3	DA2 ^{a,b}	DA 1.5
Lan 019	19 33 49.9	+18 52 03.1	10	-10	15.5	-0.9	15.4	15.7	15.8	Hot, high gravity? ^c	DA 1.0
Lan 020	19 43 31.2	+18 24 35.2	3.3	-43.8		< -0.8	12.1	12.5	12.7	sdO ^d	sdO
Lan 021	19 44 59.1	+22 45 49.2	-8	-16	16	-0.9	15.4	16.2	17.4	Hot, high gravity? ^c	DA 1.0
Lan 022	20 00 21.6	+19 07 41.1	0	0	14.7		15.2	14.8	14.9	O7-O9 ^c	DA 3.5
Lan 024	01 24 05.1	+69 13 20.3	94	-10	19	-0.6	17.0	17.2	16.3		DA 4.0
Lan 029	03 17 51.6	+53 04 20.0	-14	-16	17	-0.6	17.4	17.6	17.5		DA 2.0
Lan 057	03 10 03.2	+53 09 24.5	28	-70	17	-0.3	16.6	16.2	17.2		DC 4
Lan 062	03 31 18.1	+53 03 52.0	-18	-2	17	-0.3	16.8	17.0	17.0		DA 3.0
Lan 082	21 26 24.9	+55 13 29.3	268	192	14	-0.3	15.7	15.0	14.8	DA4 ^a	DA 3.5
Lan 126	23 39 10.5	+66 51 45.6	44	-8	19.5	-0.8	16.8	17.3	18.2		DA 4.0
Lan 142	02 28 50.0	+68 35 37.9	14	-50	17.2	-0.7	17.6	18.0	18.3		DB 3.0
Lan 143	03 03 27.8	+68 29 54.1	50	-18	16.5	-0.3	16.8	16.8	17.4		DBA 3.5
Lan 150	02 15 34.6	+64 53 22.2	44	-68	16.0	-0.5	17.8	17.0	17.5		DB 2.5
Lan 158	02 19 06.3	+70 08 39.8	36	-40	16.5	-1.0	16.6	16.6	17.1		DB 2.5
Lan 159	01 55 10.9	+69 42 41.3	-112	-6	17.0	-0.3	17.4	17.1	17.3		DA 5.5
Lan 161	01 19 41.4	+68 51 10.8	-26	10	18.0	-0.5	17.8	17.2	16.1		DA 3.0
Lan 163	01 33 38.3	+68 03 32.7	-34	-18	16.5	-0.5	17.6	16.8	16.9		DA 1.5
Lan 174	03 41 17.1	+62 42 03.1	2	-18	16.8	-0.7	17.1	17.2	17.6		DB 2.0
Lan 176	03 56 51.0	+62 26 20.0	10	-18	12.5	-0.2	12.6	11.2	10.8		F5 V
Lan 177	03 51 15.7	+61 52 46.4	84	-70	17.0	-0.5	16.8	17.3	17.6		DC 5
Lan 188	04 16 02.5	+59 44 02.4	6	-22	17.5	-0.6	17.8	18.2	18.5		DA 2.0
Lan 191	04 04 23.8	+58 58 36.2	-14	8	16.8	-0.3	17.6	17.5	17.8		DA 5.0
Lan 197	00 53 01.7	+59 59 42.6	-76	8	15.0	-0.6	16.4	16.2	15.8		DA 1.5
Lan 253	00 33 40.7	+55 51 47.0	14	-14	14.8	-0.6	16.6	16.5	15.6		DA 2.5
Lan 272	02 57 45.1	+60 34 27.4	10	-12	14.0	-0.5	15.4	15.4	15.9	PN ^f	DAO 0.5
Lan 273	03 08 18.4	+60 35 30.1	14	-74	17.0	-0.6	17.6	17.3	17.2		DA 4.0
Lan 280	02 48 41.3	+59 16 12.4	44	-118	16.5	-0.7	16.3	16.1	16.6		DA 2.5
Lan 284	03 04 17.9	+58 44 05.2	-36	-22	17.0	-1.2	16.5	16.6	17.0		DA 2.5
Lan 351	04 06 07.1	+54 31 33.9	-90	16	14.5	-0.6	15.6	15.5	15.5	DA3 ^a	DA 3.0
Lan 356	20 24 33.0	+41 23 37.2	16	12	17.0	-0.4	17.3	17.1	17.6		DA 2.5
Lan 361	20 48 08.3	+39 51 38.3	-36	-34	14.0	-0.9	14.8	14.5	14.2	DA ^a	DA 1.0
Lan 364	20 56 37.2	+43 13 26.3	2	10	17.0	-0.2	17.8	16.5	15.9		DZ

Table 1—Continued

Name	α (J2000)	δ (J2000)	μ_α (mas yr ⁻¹)	μ_δ (mas yr ⁻¹)	m_B (mag)	$U - B$ (mag)	B_J (mag)	R_F (mag)	I_N (mag)	Sp. Type (Old)	Sp. Type (New)
Lan 367	21 04 02.6	+42 47 03.5	32	22	15.5	-0.3	16.8	16.7	16.7	B0-B3 ^c	DA 2.0
Lan 401	21 16 59.3	+60 40 30.3	18	38	11.6	-0.1	13.7	12.8	12.0	Late F-G ^c	F5 V
Lan 403	21 33 14.4	+60 48 30.4	24	16	17.3	-0.6	17.7	17.7	17:		DA 2.5
Lan 406	21 24 44.9	+60 35 17.5	8	12	12.4	-0.1	14.2	13.0	11.9		F6 V
Lan 423	21 42 14.7	+58 54 01.7	-14	-2	16.5	-0.4	16.5	15.3	14.2	Early-B ^c	sdF5
Lan 432	21 58 32.5	+58 04 33.4	-6	-70	18.5	-0.6	17.4	17.2	16.9		sdB
Lan 459	22 05 38.2	+62 24 35.7	-38	10	16.0	-0.8	17.1	17.5	17.7	DA ^{a,c}	DA 1.5
Lan 480	03 29 05.7	+64 04 42.9	29.6	-11.2	11.3	-0.9	13.2	13.2	13.2	sdO ^e	sdOB
Lan 486	03 24 31.3	+62 50 53.8	-24	0	15.3	-0.7	15.8	16.1	16.5		DA 3.0
Lan 489	03 00 37.2	+62 28 27.9	6	30	16.8	-0.5	16.3	16.6	16.9		DC 5
Lan 532	04 12 42.9	+40 41 26.5	14	-44	16.0	-0.7	16.4	16.9	17.0		DA 1.5
Lan 572	04 44 50.1	+39 15 19.7	-26	-44	17.0	-0.5	17.1	17.5	17.5		DA 3.5

^aMcCook & Sion (1999).

^bLiebert & Strittmatter (1977).

^cEracleous et al. (2002).

^dWalker (1981).

^eKilkenny, Heber, & Drilling (1988).

^fChromey (1979).

Table 2. Atmospheric Parameters of DA Stars

Name	T_e	(K)	$\log g$	M_\odot	M_V	$\log L_\odot$	V_{phot}	$D(\text{pc})$	$\log \tau$
Lan 004	28640	(422)	7.33 (0.05)	0.38 (0.01)	9.00	-0.53	16.08	261	7.04
Lan 018	30350	(443)	7.96 (0.05)	0.63 (0.03)	9.87	-0.84	12.99	42	7.02
Lan 019	77680	(2732)	7.77 (0.13)	0.66 (0.04)	8.26	+1.00	15.54	285	5.77
Lan 021	55570	(1387)	7.64 (0.09)	0.56 (0.03)	8.41	+0.48	15.77	296	6.19
Lan 022	14350	(247)	7.95 (0.05)	0.58 (0.03)	11.29	-2.17	15.02	55	8.32
Lan 024	12180	(317)	8.26 (0.09)	0.77 (0.06)	12.03	-2.64	17.09	103	8.72
Lan 029	26780	(518)	8.40 (0.07)	0.88 (0.05)	10.86	-1.35	17.49	212	7.76
Lan 062	17330	(308)	8.09 (0.05)	0.67 (0.03)	11.16	-1.92	16.89	140	8.16
Lan 082	14800	(387)	8.46 (0.05)	0.90 (0.03)	12.01	-2.43	15.38	47	8.63
Lan 126	12380	(315)	8.22 (0.09)	0.74 (0.05)	11.93	-2.58	17.03	104	8.67
Lan 159	9050	(179)	8.32 (0.17)	0.80 (0.11)	13.08	-3.20	17.26	68	9.11
Lan 161	16600	(985)	8.39 (0.16)	0.86 (0.10)	11.70	-2.18	17.52	145	8.45
Lan 163	31810	(630)	7.25 (0.11)	0.37 (0.03)	8.61	-0.28	17.23	530	6.46
Lan 188	25160	(1542)	8.27 (0.23)	0.80 (0.14)	10.78	-1.38	17.98	276	7.71
Lan 191	9870	(194)	8.43 (0.14)	0.87 (0.09)	12.93	-3.12	17.55	84	9.10
Lan 197	32290	(489)	7.88 (0.06)	0.59 (0.03)	9.61	-0.67	16.31	218	6.88
Lan 253	20260	(334)	7.95 (0.05)	0.60 (0.03)	10.68	-1.56	16.55	149	7.76
Lan 272 ^a	90410	(2757)	6.99 (0.13)	0.51 (0.03)	6.30	+1.93	15.40	659	4.44
Lan 273	12960	(442)	7.93 (0.11)	0.57 (0.06)	11.45	-2.33	17.46	159	8.44
Lan 280	19020	(379)	7.73 (0.06)	0.48 (0.03)	10.46	-1.53	16.21	140	7.72
Lan 284	20280	(532)	8.12 (0.08)	0.70 (0.05)	10.94	-1.66	16.55	132	7.94
Lan 351	16750	(261)	8.08 (0.05)	0.66 (0.03)	11.19	-1.97	15.55	74	8.20
Lan 356	24590	(486)	8.31 (0.06)	0.82 (0.04)	10.88	-1.44	17.21	184	7.80
Lan 361	66320	(1396)	7.98 (0.07)	0.72 (0.03)	8.85	+0.55	14.66	145	6.00
Lan 367	25230	(461)	8.17 (0.06)	0.73 (0.04)	10.61	-1.30	16.75	169	7.55
Lan 403	19250	(450)	8.39 (0.07)	0.86 (0.05)	11.45	-1.92	17.70	178	8.26
Lan 459	29650	(704)	7.67 (0.12)	0.49 (0.05)	9.48	-0.70	17.28	364	6.98
Lan 486	17600	(396)	8.11 (0.07)	0.68 (0.04)	11.16	-1.90	15.94	90	8.15
Lan 532	34040	(536)	8.62 (0.06)	1.02 (0.04)	10.78	-1.09	16.63	148	7.68
Lan 572	14050	(817)	8.22 (0.09)	0.75 (0.06)	11.72	-2.37	17.28	129	8.53

^aThis object is a DAO star with $\log \text{He}/\text{H} = -1.4$.

Table 3. Atmospheric Parameters of DB and DBA Stars

Name	T_e	(K)	$\log g$	$\log \text{H}/\text{He}$	M_\odot	M_V	$\log L_\odot$	V_{phot}	$D(\text{pc})$	$\log \tau$
Lan 142	18020	(507)	8.23 (0.16)	-5.08 (0.37) ^a	0.74 (0.10)	11.24	-1.95	17.78	203	8.23
Lan 143	15240	(285)	8.66 (0.11)	-3.71 (0.04)	1.01 (0.06)	12.36	-2.53	16.80	77	8.75
Lan 150	21000	(855)	7.97 (0.09)	-6.50 (0.00) ^a	0.59 (0.05)	10.57	-1.52	17.43	235	7.76
Lan 158	21930	(1309)	7.92 (0.10)	-4.32 (0.36) ^a	0.56 (0.05)	10.44	-1.41	16.60	170	7.61
Lan 174	22400	(1987)	7.33 (0.23)	-4.59 (0.86) ^a	0.33 (0.06)	9.61	-1.02	17.15	321	7.56

^aUpper limit based on the absence of $\text{H}\alpha$.